JOURNAL OF AIRCRAFT
Vol. 30, No. 3, May–June 1993

Integrated Structure/Control/Aerodynamic Synthesis of Actively Controlled Composite Wings

E. Livne*
University of Washington, Seattle, Washington 98195
and
L. A. Schmit† and P. P. Friedmann‡
University of California, Los Angeles, Los Angeles, California 90024

A new multidisciplinary optimization capability for integrated synthesis of actively controlled composite wings is reviewed. It is shown that the nonlinear programming/approximation concepts approach to design optimization, combined with appropriate simplified analysis techniques for the different disciplines, make multidisciplinary wing synthesis both feasible and practical for the conceptual and preliminary design stages. The composite wing of a remotely piloted vehicle is used for numerical experimentation. Synthesis studies with design variables and constraints that span the disciplines of structures, control, and aerodynamics are presented. These studies provide new insight into the complex nature of multidisciplinary interactions in wing design.

Nomenclature

$[\tilde{A}]$, $\{\tilde{B}\}$ = aeroservoelastic system state space matrix and input vector in standard form
$[A_D]$ = aerodynamic matrix used for the calculation of induced drag
$a_c, b_c, c_c, d_c, e_c, f_c$ = control system design variables (coefficients in the transfer function of a control law)
D_I = induced drag
$D_{I(\text{APPRX})}$ = induced drag approximation
I_t = number of terms in the thickness polynomial for $t(x, y)$
I_w = number of terms in the Ritz polynomial series for elastic deformation $w(x, y)$
I_0 = number of terms in the polynomial series for jig shape
$[K]$ = structural generalized stiffness matrix
$[\tilde{K}]$ = aeroelastic (structural and aerodynamic) generalized stiffness matrix
$\{P\}$ = generalized static loads
$\{\tilde{P}\}$ = generalized loads in maneuver (including inertial, jig shape, and control surface contributions)
$\{q\}$ = static generalized displacements
$\{\tilde{q}\}$ = generalized displacements in maneuver (including control surface rotation needed)
$\{q_{\text{APRX}}\}$ = approximate generalized displacements in maneuver
$\{q_c\}$ = vector of control surface rotations
$\{\dot{q}_c\}$ = vector of control surface rotation rates
$\{q^0\}$ = generalized displacements defining the jig shape of the wing
S = reference area
s = Laplace variable
T_i = coefficients of the thickness polynomial, Eq. (9)
$t(x, y)$ = skin layer thickness distribution
U = speed of flight
$[U]$, $[V]$, $\{W\}$ = state space aeroservoelastic system matrices and gust input vector
$\hat{w}$ = zero mean Gaussian white noise input
$w(x, y, t)$ = wing elastic vertical deformation
$\ddot{w}_{0.65c}$ = actual vertical acceleration at 65% of the wing chord containing the flutter suppression control surface
$[X]$ = state covariance matrix of aeroservoelastic response to a white noise input
$\{x(s)\}$ = Laplace transformed state vector of the aeroservoelastic system
y_k = a typical output of the aeroservoelastic system
y_{SE} = accelerometer output
$\{\delta\}$ = vector of flap rotation settings
δ_c = control command
ζ_{ic}, ω_{ic} = damping and natural frequency associated with a second-order filter in the control law, Eqs. (14–18)
$\dot{\theta}$ = pitch rate in maneuver

Introduction

APPLICATION of composite materials technology and high authority control systems to the design of actively controlled, light weight, flexible wings[1,2] has made the interactions among the various disciplines in airplane design more complex and important.[3–6] Failure to take these interactions into account can lead to potentially disastrous consequences.[7] On the other hand, taking advantage of them early in the design process, offers greater design flexibility leading to improved designs.[8,9] The integrated treatment of structures, control systems, flight mechanics, performance, and dynamic aeroelasticity has therefore become a necessity.[10]

A growing body of research on the multidisciplinary synthesis of wings is indicative of this need for integrated design tools. Integrated structure/aerodynamic,[11] structure/control,[12] and aerodynamic/control[13] design studies are representative recent examples. The problem is computationally intensive and can be approached in various ways. One approach is based on decomposition techniques as a strategy for large-scale optimization. Some studies choose to focus only on se-

Received March 9, 1991; revision received Feb. 19, 1992; accepted for publication Feb. 25, 1992.

*Assistant Professor, Department of Aeronautics and Astronautics. Senior Member AIAA.
†Rockwell Professor of Aerospace Engineering, Emeritus, Mechanical, Aerospace, and Nuclear Engineering Department. Fellow AIAA.
‡Professor of Engineering and Applied Science, Department of Mechanical, Aerospace, and Nuclear Engineering. Fellow AIAA.

lected aspects of the problem. Others use simplified mathematical models in an effort to gain insight.

In a recent series of publications[14-16] a new synthesis capability for actively controlled fiber composite wings has been described. It is based on balanced design and analysis models that capture essential behavior characteristics, without making the integrated multidisciplinary design optimization task intractable. This approach combines computationally efficient approximate analyses of the structural, aerodynamic, and aeroservoelastic behavior of composite wings used for the conceptual and preliminary design stages. The entire optimization problem can be treated at a single level without the need for multilevel decomposition.

Exploratory studies in actively controlled wing multidisciplinary optimization were presented in Ref. 15. They focused on the integration of controls and structure in aeroservoelastic design optimization. The interaction between a conventional metal structure of a remotely piloted vehicle (RPV) wing and the active flutter suppression/gust alleviation system was studied. Structural and control system sizing type design variables[14,16] were included in the design space. Tradeoffs between structural mass and required control system power were examined.

The purpose of this article is to report the results of new, more comprehensive, multidisciplinary wing synthesis studies made possible by the new synthesis capability. The RPV model used in Ref. 15 serves as a test case again. Structural design freedom is increased by introducing fiber composite materials for wing skin construction. The design space is expanded further by adding aerodynamic design variables (to determine the jig shape of the wing). Induced drag constraints are added to the set of constraints. Therefore, the design space spans three disciplines: 1) structures, 2) controls, and 3) aerodynamics; and the combination of behavior constraints covers strength, minimum gauge, flutter, gust response, and performance (through induced drag) requirements.

The design studies considered are unique. The state of the art in design optimization is advanced by the development and application of synthesis techniques suitable for complex multidisciplinary problems involving a rich blend of constraints. In addition, better understanding of the complex interactions between the various disciplines in wing design emerge, and the numerical results obtained provide a basis for design tradeoffs.

Analytical Modeling Techniques

The selection of modeling techniques was guided by the need to bridge the gap between those that are simple, and detailed techniques that require too much computer time. In the structures area, an equivalent plate analysis (Fig. 1) is used.[16-18] This technique lacks the generality and accuracy of the finite-element method, especially when localized effects are considered. However, as shown in Refs. 17–20 equivalent plate analysis predicts overall static deformation and free vibration characteristics of typical low-aspect ratio airplane wings quite accurately. Furthermore, as shown in Refs. 16 and 17, the equivalent plate method can also generate adequate approximations for skin and spar cap stresses. In terms of CPU time required, equivalent plate analysis is much faster than the alternative finite-element analysis. In some cases—by an order of magnitude.

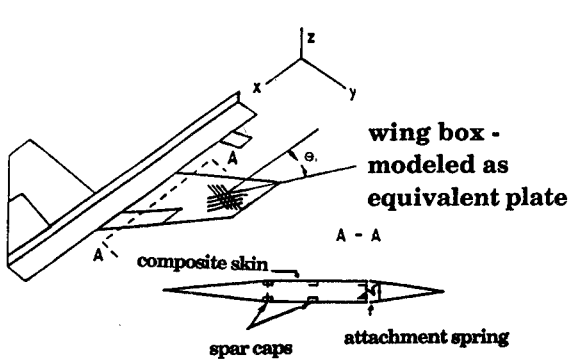

Fig. 1 Airplane as an assembly of equivalent plates.

The equivalent plate structural analysis of Ref. 16 is then combined with the piecewise continuous kernel function method (PCKFM) unsteady aerodynamics for lifting surfaces.[21] The method of Roger[22] is used to generate finite-dimensional state space approximations for the unsteady aerodynamic loads. The integrated aeroservoelastic system is assumed to be a linear time invariant (LTI) system. The control system is completely described by the location of sensors and control surfaces and by the transfer functions of the sensors, control laws, and actuators. Behavior sensitivity analysis is based on analytical derivatives of all behavior functions with respect to all design variables.

Analysis Capabilities

Static "Maneuver Load" Analysis

Static aeroelastic deflections and stresses are calculated for the elastic airplane in maneuver. Maneuvers include symmetric pull-ups (defined by Mach number, altitude, and load factor) or steady rolling maneuvers (defined by Mach number, altitude, and roll rate). In addition to elastic deflections and stresses, the control surface deflections and hinge moments needed for the maneuvers are obtained. Maneuver deflection and stress analysis consists of solving the equations of motion of the free-free deformable airplane during a maneuver. When using a stiffness formulation based on the Ritz polynomial functions to approximate elastic deformations in the equivalent plate approach[16-18] these equations are

$$[\tilde{K}]\{\tilde{q}\} = \{\tilde{P}\} \tag{1}$$

where $\{\tilde{q}\}$ is a vector of generalized displacements including an added control surface rotation degree of freedom (DOF) needed for pull-up or roll. The matrix $[\tilde{K}]$ is a nonsymmetric matrix whose elements are combinations of structural stiffness, aerodynamic stiffness, and aerodynamic control surface stiffness terms. The vector $\{\tilde{P}\}$ depends on inertial forces, jig shape aerodynamic effects, and rotation setting of additional control surfaces for drag or load modification.

Static "Preassigned Load" Analysis

Static deflections and stresses are calculated for the cantilevered wing under a set of prescribed loads. This option can be important for loads due to higher angles of attack where the linear aerodynamic theory used for maneuver loads is inadequate. For such cases, loads based on wind-tunnel data or CFD computations can be used. The displacement formulation of linear structural analysis leads to

$$[K]\{q\} = \{P\} \tag{2}$$

where $[K]$ is the symmetric structural generalized stiffness matrix associated with the Ritz generalized displacements $\{q\}$.

Free Vibration Analysis

Natural frequencies and mode shapes are obtained for different sets of boundary conditions. Cantilevered and free-free symmetric or antisymmetric modes can be generated for use as basis vectors leading to reduced order structural models for aeroservoelastic analysis. Constraints can also be imposed on one or more natural frequencies directly.

Aeroservoelastic Stability Analysis

Poles of the LTI state space model of the control augmented airplane are calculated for different flight conditions and boundary conditions (cantilevered or free-free symmetric and antisymmetric motion). Detailed discussion and derivation of

relevant equations are given in Refs. 14 and 16. Assembly of the state space models of the structure, sensors, actuators, control laws, as well as approximate unsteady air load and gust aerodynamics, leads to the closed loop state space equations of the complete system in the form[14-16]

$$s[U]\{x(s)\} = [V]\{x(s)\} + \{W\}\hat{w} \tag{3}$$

A "gust filter" is used to transform $\hat{w}$ into a vertical gust speed of given power spectral density and root mean square (rms) value that actually excites the structure during flight in turbulence. In Eq. (3) s is the Laplace variable and the state vector $\{x\}$ contains structural, sensor, actuator, control law, gust filter, and aerodynamic states. The system matrices $[U]$ and $[V]$ depend on structural and control system design variables.

Gust Response Analysis

The rms values of control surface rotations and rotation rates as well as rms values of selected sensor measurements due to continuous atmospheric turbulence are calculated for different flight conditions. Both Dryden and rational approximations for the Von-Karman turbulence spectra are implemented. The relevant quantities are rms values of control surface rotations $\{q_c\}$, rates $\{\dot{q}_c\}$ and sensor measurements $\{y_{SE}\}$. Premultiplication by $[U]^{-1}$ transforms the state space equations [Eq. (3)] into the standard form

$$s\{x(s)\} = [\tilde{A}]\{x(s)\} + \{\tilde{B}\}\hat{w}(s) \tag{4}$$

A stationary random process is assumed,[23] and rms values of elements of $\{q_c\}$, $\{\dot{q}_c\}$ and $\{y_{SE}\}$ are found using the state covariance matrix $[X]$. The state covariance matrix is a solution of a Lyapunov's matrix equation[23] in the form

$$[\tilde{A}][X] + [X][\tilde{A}]^T = -\{\tilde{B}\}[Q_w]\{\tilde{B}\}^T \tag{5}$$

where $[Q_w]$ is the intensity matrix of the Gaussian white noise $\hat{w}$. The Hessenberg-Schur method[24] is used to solve Eq. (5).

Induced Drag Analysis

Typical examples of the application of optimization techniques to induced drag reduction aimed at the generation of desirable twist and camber distributions are described in Refs. 25-27. Desirable initial twist and camber (jig shape), combined with aeroelastic tailoring to control elastic deformations in flight and maneuver-dependent deflection of flaps, can all be quite effective. Once the jig shape, elastic deformation, and flap deflections are known, several methods based on lifting surface aerodynamic theory[25-30] can be used for the calculation of induced drag (assuming small angles of attack, small deformations, and small flap deflections). The lifting surface PCKFM[28] is used in the new capability, and drag can be calculated assuming either full leading-edge suction (fully attached flow) or no leading-edge suction (separated flow at the leading edge) or a combination of these. The subsonic induced drag D_I is expressed in quadratic form (Ref. 16)

$$D_I = \tfrac{1}{2}\rho U^2 S\{\bar{q}\}^T[A_D]\{\bar{q}\} \tag{6}$$

where $\frac{1}{2}\rho U^2$ is the dynamic pressure, S is a reference area, and $[A_D]$ is an aerodynamic matrix. When the displacements and control surface rotations are small, then (within linearized lifting surface theory) this matrix is fixed and does not depend on either structural or aerodynamic design variables.[25] It is generated once for the set of deflection Ritz polynomials, control surface rotations, and downwash due to pitch rate DOF in symmetric pull-up maneuvers. The vector $\{\bar{q}\}$ is defined as follows

$$\{\bar{q}\} = \begin{Bmatrix} q \\ \delta \\ 0 \end{Bmatrix} + \begin{Bmatrix} q^0 \\ 0 \\ \dot{\theta} \end{Bmatrix} \tag{7}$$

where $\{q\}$ and $\{q^0\}$ are the generalized displacements associated with elastic and initial (jig) shapes. The vector $\{\delta\}$ contains all control surface rotations and $\dot{\theta}$ is the pitch rate. Therefore, in view of Eq. (6), D_I depends on the structural and aerodynamic design variables through the generalized elastic displacements in maneuver $\{q\}$, the jig shape generalized coefficients $\{q^0\}$ and flap rotations $\{\delta\}$.

Multidisciplinary Synthesis Methodology

Optimization Strategy

Following its success in structural synthesis, the nonlinear programming approach combined with approximation concepts (NLP/AC) is used for the multidisciplinary optimization task.[31,32] In this method only a small number of detailed analyses are carried out during optimization. Each detailed analysis and the associated behavior sensitivity analysis serves as a basis for constructing explicit approximations to the objective and constraint functions in terms of the design variables. Consequently, a series of approximate optimization problems is solved until convergence to an optimal solution is achieved. Each step, consisting of detailed analysis, behavior sensitivity analysis, approximate problem generation, and a solution of the optimization problem (using approximate objective function and constraints) is an "optimization cycle." In order to prevent the approximate problem from becoming too inaccurate as the design moves from the point in design space where detailed analysis was carried out, additional constraints are added to the approximate optimization problem in a form of move limits on the design variables. Experience in structural synthesis shows that for problems involving stress, displacement, and natural frequency constraints, convergence of the synthesis process is achieved in 10-15 optimization cycles. The optimizer, of course, will need many more function and derivative evaluations, but these are based on the approximations and are computationally cheap. For the NLP/AC approach to be practical, it is crucial to avoid too many detailed analyses for actual function evaluation and derivative calculations. This depends on ensuring that the approximations are accurate, yet simple enough for efficient solution.

Design Variables

Preassigned parameters for the optimization include wing planform and depth distribution, material properties, and structural layout of the wing (number of spars and ribs and their locations). Control system architecture is also preassigned. Thus, the number of sensors and actuators and their locations are given together with the number of control laws transforming given combinations of sensor outputs into control commands. It is also assumed that the order of the transfer functions for sensors, actuators, and control laws is given and cannot be changed during optimization. To take advantage of multidisciplinary interactions, the design space includes structural, control system, and aerodynamic design variables simultaneously. Structural design variables include polynomial coefficients T_i in the series describing skin layer thickness distribution $t(x, y)$ over the wing

$$t(x, y) = \sum_{i=1}^{I_t} T_i x^{m_i} y^{n_i} \tag{8}$$

Additional structural design variables include spar/rib cap areas, concentrated masses, and spring constants (for the springs representing stiffness of actuator and backup structure connecting control surfaces to the wing box or canard to the fuselage). Control system design variables include polynomial coefficients $b_0, b_1, \ldots, b_n$ and $d_0, d_1 \ldots, d_{n-1}$ in the transfer functions representing control laws of the form

$$\frac{\delta_c}{y_{SE}} = \frac{b_n s^n + b_{n-1}s^{n-1} + \cdots + b_1 s + b_0}{s^n + d_{n-1}s^{n-1} + \cdots + d_1 s + d_0} \tag{9}$$

where δ_c is the control command. Aerodynamic design variables include coefficients in the polynomial series for wing initial (jig) shape

$$w_0(x, y) = \sum_{i=1}^{I_{W0}} q_i^0 x^{r_i} y^{s_i} \tag{10}$$

and flap rotation settings δ. The shape polynomials used for the jig shape are taken to be identical to the Ritz polynomials used for wing elastic deflection

$$w(x, y, t) = \sum_{i=1}^{I_w} q_i(t) x^{r_i} y^{s_i} \tag{11}$$

Following the hierarchy of Ref. 14, the control augmented structural synthesis problem formulated in this work is a sizing problem for the disciplines. Sizing type design variables are included in the design space, whereas, shape and topological design variables are preassigned. Thus, the balanced treatment of analysis in three disciplines (controls, aerodynamics, and structures) is also retained in formulating the optimization problem.

Objective Functions and Behavior Constraints

A variety of constraints and objective function options are included in the new capability. The wing can be synthesized to minimize mass or gust response, or maximize performance with constraints on stresses, aeroservoelastic stability, aircraft performance (in terms of roll, rate, drag, or drag polar specifications), and control system performance (in terms of activity in gusts and limits on control surface travel and hinge moment). The objective function can be chosen to be mass, drag, rms value of any response to atmospheric turbulence (to be minimized), or steady roll rate or lift-to-drag ratio (to be maximized), or a combination of these. Constraints are imposed to satisfy a combined stress criterion for composite skin layers and a unidirectional stress criterion for spar/rib caps. The aeroservoelastic system poles are forced to reside to the left of some specified negative damping value in the complex plane, assuring a required degree of dynamic stability. If not included as part of the objective function, the drag, lift/drag, mass, or roll rate can be constrained to ensure acceptable performance. Static load conditions include sets of given loads acting on the wing or definitions of airplane maneuvers. In the second case, static deformation and stresses are calculated to take trim and aeroelastic load redistribution into account.

Behavior Function Approximations

Research during the past 15 yr has produced a variety of methods for the construction of numerically efficient approximations to important behavior functions such as elastic deformation, stress, buckling, and natural frequencies.[33–35] First-order Taylor series in the design variables (direct approximation), in the reciprocals of the design variables (reciprocal approximation), or choice of the more conservative between the two (hybrid approximation), has proved to be quite successful in structural synthesis and aeroelastic wing optimization. Extension of NLP/AC to control augmented structural synthesis made it necessary to focus attention on the poles of the combined control-structural system. Taylor series approximations and Rayleigh Quotient approximations (RQA) have been described in Refs. 37 and 38. The following behavior function approximations are available in the present capability: 1) reciprocal approximations in terms of the structural design variables are used for elastic deformations and stresses; 2) direct, reciprocal, hybrid, or RQA approximations can be used for aeroservoelastic poles; 3) direct, reciprocal, or hybrid approximations can be used for gust response constraints; and 4) direct approximations are used for the mass. The minimum gauge constraints at an array of selected points on the wing are linear in the structural design variables T_i [see Eq. (8)]. Therefore, a direct approximation of the minimum gauge constraints is in fact exact.

Induced drag constraints are quadratic in $\{\bar{q}\}$ [see Eq. (6)]. The vector $\{\bar{q}\}$ [Eq. (7)] is used as an intermediate response quantity and its approximation $\{q_{\text{APRX}}\}$ is constructed as a first-order Taylor series using reciprocal of the structural design variables (influencing $\{q\}$) and direct aerodynamic design variables ($\{q^0\}$ and δ). The explicit approximation for $\{\bar{q}\}$ is then substituted into Eq. (6) to produce the approximate induced drag:

$$D_{I_{(\text{APPRX})}} = \tfrac{1}{2}\rho U^2 S\{q_{\text{APRX}}\}^T[A_D]\{q_{\text{APRX}}\} \tag{12}$$

The quadratic nature of the induced drag is thus captured in the approximation of D_I.

RPV Wing Example

Optimization studies presented here deal with a small RPV similar to the NASA DAST research vehicle.[1,39] Its planform geometry is shown in Fig. 2. A biconvex 10% t/c wing is actively controlled by a small control surface located at about 80% semispan towards the tip. The chord of the control surface is 20% of the local wing chord, and it is driven by an actuator whose transfer function is preassigned as follows:

$$\frac{q_{c1}}{\delta_{c1}} = \frac{1.7744728 \times 10^7}{(s + 180)(s^2 + 251s + 314^2)} \tag{13}$$

where q_{c1} and δ_{c1} denote actuator actual deflection and its command, respectively. Control actuators are assumed to be irreversible.

The wing control surfaces are used only for active flutter control. The elevators are used for rigid body pitch and roll. The elevator actuator transfer function is

$$\frac{q_{c2}}{\delta_{c2}} = \frac{20}{(s + 20)} \tag{14}$$

The RPV structure is simplified for the present studies. It is modeled as an assembly of four equivalent plates. A flexible wing is attached to a rigid fuselage and rigid control surfaces. The main wing box structure, which extends from root to tip spanwise, and from leading edge to 80% chordwise, is the structure to be synthesized. The combined weight of fuselage, control surfaces, and nonstructural wing mass is 308 kgm for a half airplane. A Dryden gust model with a scale length of 518.16 m and a vertical gust rms velocity of 1.06 m/s is used. An accelerometer is placed on the wing strip containing the control surface. It is located in the middle (spanwise) and at the 0.65 chord point of the strip.[39] Its measurement serves as an input to a control law which, in turn, generates an input command δ_c to the actuator of the wing control surface. The set of three load conditions for wing stress calculations consists of 3 g symmetric pull-ups at sea level, 10,000 ft and 20,000 ft. In the maneuver load calculations the airplane is trimmed

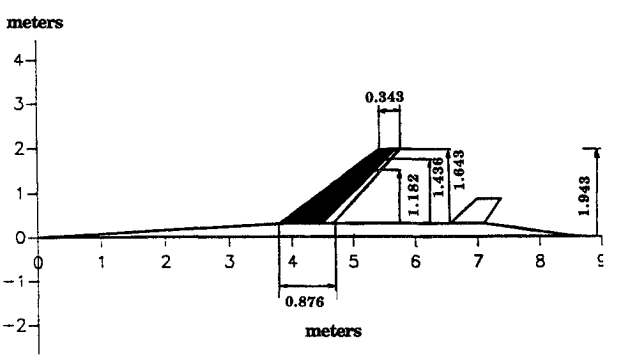

Fig. 2 Drone geometric layout.

using the elevator. All stress constraints reflect a 1.5 safety factor. Flutter, gust, and aeroservoelastic stability calculations are carried out at sea level, Mach 0.9 for the cantilevered wing. This is done intentionally in order to be able to first examine flutter suppression/structural optimization using a realistic but simple example without flight mechanics interactions.

It should be emphasized that the simplifying assumptions above are made only for illustrative purposes and to facilitate physical interpretation of the design optimization results. The present capability can handle more sophisticated airplane models where multiple equivalent plate elements are synthesized subject to several pull-up or rolling maneuvers. Control systems can obtain many control elements and control laws, and aeroservoelastic/gust response analyses can be carried out for symmetric/antisymmetric free-free motion in several flight conditions.

The control law used for this study consists of a combination of two second-order filters in parallel. This low order control law provides "local" damping in the range of frequencies where damping is needed[39] and it has the form

$$\frac{\delta_c}{y_{SE}} = \left[\frac{a_c}{(s^2 + b_c s + c_c)} + \frac{d_c}{(s^2 + e_c s + f_c)}\right] \tag{15}$$

where a_c, b_c, c_c, d_c, e_c, and f_c are control system design variables. The denominator coefficients can be associated with equivalent damping ζ_c and natural frequency ω_c of the control law for each filter

$$c_c = \omega_{1c}^2 \tag{16}$$

$$f_c = \omega_{2c}^2 \tag{17}$$

$$b_c = 2\zeta_{1c}\omega_{1c} \tag{18}$$

$$e_c = 2\zeta_{2c}\omega_{2c} \tag{19}$$

Thus, c_c, f_c, b_c, and e_c determine the center frequencies and gain peak widths of the control law transfer function while a_c and d_c determine the effective gains. The preassigned accelerometer transfer function is

$$\frac{y_{SE}}{\ddot{w}_{0.65c}} = \frac{314^2}{(s^2 + 376.8s + 314^2)} \tag{20}$$

where $\ddot{w}_{0.65c}$ denotes the actual vertical acceleration at the measurement point.

The RPV wing box skins are made of glass/epoxy laminates. Fibers are oriented at 0, 90, +45, and −45 deg relative to a line passing through the midchord points of the wing box. Thus, the skin model consists of four unidirectional lamina. The thickness distribution of each of these lamina is described by a nine term polynomial in x and y

$$t(x, y) = T_1 + T_2x + T_3x^2 + T_4y + T_5yx + T_6yx^2 + T_7y^2 + T_8y^2x + T_9y^2x^2 \tag{21}$$

Therefore, there are 36 structural design variables T_i and six control system design variables, a_c to f_c, when the control system is included. When aerodynamic design variables are added, they consist of the coefficients of a polynomial in x and y defining the jig shape of the wing [Eq. (10)]. A six-term second-order complete polynomial was used.

The nonlinear programming algorithm used for constrained function minimization throughout this study is the method of feasible directions as implemented in the CONMIN code.[40,41]

Results and Discussion

Structural Designs

Minimum weight designs using only the structural design variables subject to minimum gauge and stress constraints ("stress design") or subject to gauge, stress, and flutter constraints ("flutter design") are synthesized first (Fig. 3). The flutter constraints are in the form of a 2% lower bound on viscous damping in five modes corresponding to the lowest frequencies. The optimization is started with a uniform skin thickness. Figure 3 shows the variation of skin mass with the number of optimization cycles. The stress design is found to be aeroelastically unstable at the flutter design flight condition (sea level, $M = 0.9$). As expected, when flutter constraints are added to the stress and minimum gauge constraints, the resulting design is heavier reflecting the need to stiffen the wing. Design variable move limits of 40% were used and convergence was achieved within 15 optimization cycles.

Structure/Control Designs

Next, the control system is introduced and wing mass is minimized subject to gauge, stress, and flutter constraints, whereas, the design space includes 36 structural and 6 control system design variables. The mass iteration history for this case is shown in Fig. 4 and it is denoted by "gauge + stress + flutter constraints." Through simultaneous changes in structural and control law design variables, a final minimum mass design which satisfies all constraints is obtained. The active control system, using the fourth-order control law, makes it possible to stabilize the wing without any structural mass penalty when compared to the unstable stress design. This is not unexpected, since an unstable plant can be stabilized with the addition of a properly designed control system (assuming stabilizability). However, in the classical approach to control system design, the plant is given and the designer focuses on synthesizing a control system. Here, the plant and the control system are synthesized simultaneously.

Addition of an active control system to the wing adds weight and cost. These are usually correlated with the required control system power (and, traditionally in aeroservoelasticity,

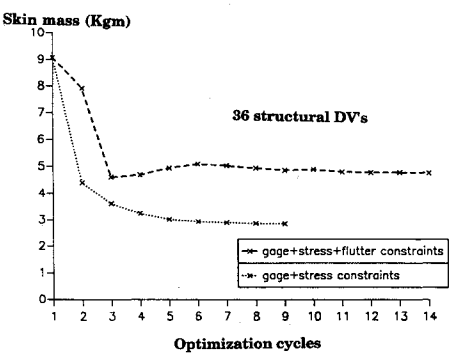

Fig. 3 Stress and flutter skin mass design histories—RPV composite wing.

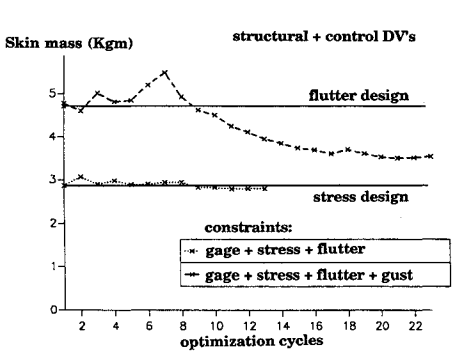

Fig. 4 Skin mass histories with and without gust response constraints.

with rms of aileron rotation and rate of rotation in atmospheric turbulence). Constraints on required control system power must therefore be included in any control system design.

Freezing the stress design (unstable) of the composite RPV wing and looking for the "best" control system to stabilize it using a fourth-order control law leads to the design history shown in Fig. 5. This follows a typical sequential approach to design where first the structure is optimized and then some optimal control system is synthesized to fix any aeroservoelastic problems. Six control system design variables are now used in an effort to find a control system with minimum rms of aileron rotation due to atmospheric gusts. Ten percent design variable move limits are used to converge to a control law which yields a minimum rms rotation of 1.9 deg and associated rms of rotation rate of 249 deg/s. During the optimization, when stability is lost, the gust response calculation is bypassed. This manifests itself as a gap in the design history in Fig. 5. The optimizer (CONMIN) then focuses on finding a feasible (stable) design[40] before gust response calculations resume. If more stringent constraints on the control system are imposed (limit the rms of control surface rotation in turbulence to less than 1.9 deg) it is necessary to trade in some structural weight as shown in Fig. 4. The design history denoted "gauge + stress + flutter + gust" corresponds to skin mass minimization subject to added constraints on the rms rotation and rate of rotation of the aileron in turbulence so that these are less than or equal to 0.95 deg rms and 95 deg/s rms, respectively (considerably lower than the 1.9 deg and 249 deg/s with the control system optimized for the given stress design).

In other words, a control system with a given structure whose power requirements are constrained to be below a certain limit cannot stabilize the present stress design unless some weight penalty is introduced because of the need to modify the structure itself. In this case, the control system and the plant have to be synthesized simultaneously in order to arrive at a feasible improved design. Of course, it might be argued that control system power implies added mass, and that for the tradeoff studies to be more realistic, we need to include the weight of the control system in the objective function. The current capability can take this into account by linking the values of certain concentrated masses to the rms aileron rotation and rotation rate needed. This capability, however, was not used in the examples presented here. Nevertheless, the complex tradeoff between structural weight and control system power (or the resulting weight of the control system) is evident.

Structure/Control/Aerodynamic Design Studies

References 8 and 9 have demonstrated the effectiveness of aeroelastic tailoring in reducing the induced drag of fiber composite wings. Starting with the RPV composite wing box stress design (Fig. 3), minimum weight designs are now sought subject to the previous stress and gauge constraints plus induced drag constraints. The induced drag coefficients of the stress design at 0, 10,000 and 20,000 ft at $M = 0.9$ serve as a reference. Drag reductions of increasing magnitudes are imposed in a series of weight minimizations and the resulting skin masses are shown in Fig. 6. The trend here is essentially the same as the one reported in Ref. 9. Additional weight is used to achieve the elastic deformation in maneuver that will yield the desired reduction in drag. There is a limit, however, to the drag reduction feasible with aeroelastic tailoring only. In the present example, drag reductions of more than 3.0% could not be achieved. To achieve further reductions in drag, aerodynamic design variables (jig shape, flap rotations) must be added.[9] Figure 7 shows the mass of minimum weight designs subject to a drag reduction of 2.5% relative to the reference stress design. With only structural design variables subject to drag, stress, and minimum gauge constraints, the resulting skin mass is 3.12 kgm. The wing is unstable, however, and when a flutter constraint is added the minimum mass almost doubles to 6.17 kgm. This is an interesting result. Apparently the structure can only satisfy both drag and flutter requirements with a substantial weight increase. When the active control system is added and the control system design variables are included in the design space, the minimum mass structural weight which satisfies all stress, gauge, flutter, and drag constraints is 3.19 kgm. The structure is tailored then to take care of the stress and drag constraints while the control system stabilizes the wing and takes care of flutter. This last design is still heavier than the stress design because of the need for the structure to take care of the drag constraint. A set of aerodynamic design variables is now added to the design space. They determine the jig shape of the wing and consist of six coefficients in a complete second-order polynomial for the initial shape $w_0(x, y)$ [Eq. (10)]. The skin mass is now minimized subject to gauge, stress, flutter, and induced drag constraints. Forty-eight design variables are now used: 36 structural design variables controlling the thickness of four skin laminates, 6 control system design variables in the fourth-order control law, and 6 aerodynamic jig shape variables. The skin mass design history is shown in Fig. 8. With the addition of aerodynamic design variables, the minimum weight is brought down to a value that is only 3% higher than the stress design

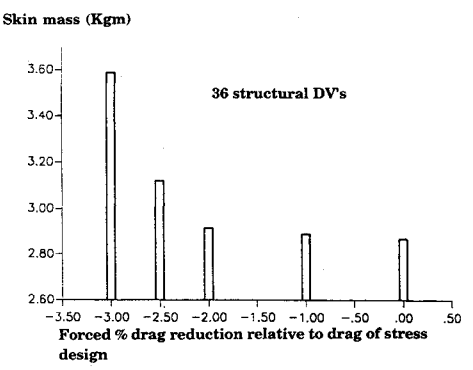

Fig. 6 RPV minimum skin weights with stress, gauge, and varying stringency of induced drag constrains.

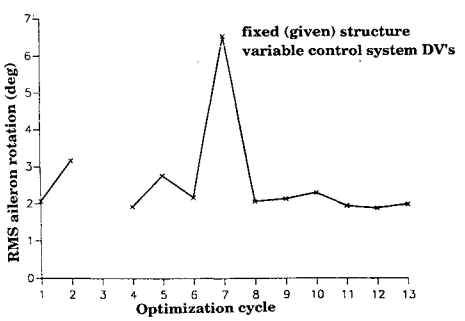

Fig. 5 History of aileron gust rms rotation during minimization with control system design variables.

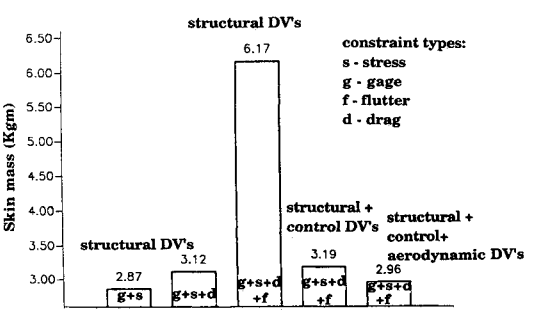

Fig. 7 Minimum mass designs for 2.5% induced drag reduction relative to the stress design.

Table 1 Wing tip elastic twist in symmetric pull-up

Constraints[a]	$s + g$	$f + g$	$g + s + d$	$g + s + d + f$	$g + s + d + f$
DVs	Structural	Structural	Structural	Structural	Structural + control + jig shape
Washout, deg	1.0793	1.3434	0.9616	0.7311	0.9677

[a] g = Gauge, s = stress, f = flutter, and d = drag. Minimum skin mass designs; positive-for washout.

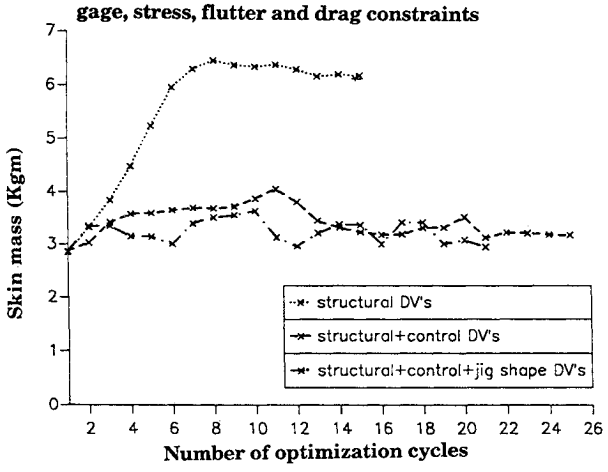

Fig. 8 Skin mass histories with different types of design variables.

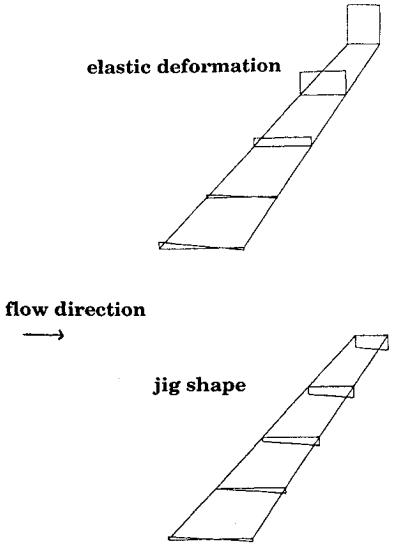

Fig. 9 Jig shape and elastic deformation in maneuver for minimum weight wing design with structural, control, and aerodynamic design variables.

weight. This is intuitively rewarding, since now the jig shape helps take care of the drag constraint, the control system prevents flutter, and the structure is tailored primarily for gauge and stress constraints.

The experience gained so far with the current capability suggests the following move limits on design variables (DVs) for acceptable constraint approximation accuracy and optimization convergence. When only structural DVs are used subject to gauge, stress, and flutter constraints, move limits of 40% were satisfactory. The addition of drag constraints made it necessary to reduce move limits on structural DVs to 20%. When control system DVs are added with corresponding aeroservoelastic stability and gust response constraints, move limits on these DVs were 10%. With these tight move limits RQA and reciprocal first-order Taylor series approximations produced similar results. A typical synthesis of structure, control, and jig shape subject to 1430 constraints and involving 42 DVs (spanning structure, control, and aerodynamics) took 54 min of CPU time on the UCLA IBM 3090 Model 600J.

Additional insight into the complex multidisciplinary interactions can be obtained by examining Fig. 9 and Table 1. Figure 9 shows the composite wing jig shape and its elastic deformation in a 3 g, sea level, $M = 0.9$ pull-up maneuver for the design obtained using structural, control, and jig shape design variables. The root angle of attack reflects the rigid body angle of attack needed. Elastic wing twist is obtained by subtracting the tip angle of attack from the root angle of attack. Positive values of twist angle are used to denote wash-out (leading edge down-reduced tip load) deflection. In Table 1 it is interesting to observe the need for more wash-out in the case of structural flutter design and less wash-out in the case of structural drag design when compared with the stress design. These conflicting requirements may explain the substantial weight penalty associated with the requirement to satisfy drag and flutter constraints simultaneously. When jig shape and control system design variables are added, flutter is taken care of by the control system while the jig shape introduces wash-in (leading edge nose up) to effectively reduce the total wash-out compared with the stress design to a level similar to the wash-out in the drag design.

Concluding Remarks

The accumulated experience with the new methodology for wing synthesis described here demonstrates that single level integrated multidisciplinary synthesis of realistic wing models (including constraints and design variables in structures, control, and aerodynamics) is both feasible and practical. These numerical experiments, carried out with the multidisciplinary synthesis capability reported in Ref. 16, provided interesting insight into the complex nature of multidisciplinary interactions present in modern wing design. The interpretations of synthesis results offered in this article should be taken with caution since they may be problem dependent. However, the results reported here clearly indicate that NLP/AC synthesis methodology provides a powerful tool for conducting the kind of quantitative tradeoff studies needed to design superior actively controlled fiber composite wings.

Acknowledgment

This research was supported by AFOSR Contract F 49620-87-K-0003.

References

[1]Newsom, J. R., Adams, W. M., Mukhopadhyay, V., Tiffany, S. H., and Abel, I., "Active Controls: A Look at Analytical Methods and Associated Tools," *Proceedings of the 14th Congress of the International Council of the Aeronautical Sciences*, ICAS-84-4.2.3, Toulouse, France, 1984, pp. 230–242.

[2]Weisshaar, T. A., "Aeroelastic Tailoring—Creative Uses of Unusual Materials," AIAA/ASME/ASCE/AHS 28th Structures Structural Dynamics and Materials Conf., AIAA Paper 87-0976-CP, Monterey, CA, April 6–8, 1987.

[3]Rimer, M., Chipman, R., and Muniz, B., "Control of a Forward Swept Wing Configuration Dominated by Flight Dynamics/Aeroelastic Interactions," *Journal of Guidance, Control, and Dynamics*, Vol. 9, No. 1, 1986, pp. 72–79.

[4]Beaufrere, H., "Limitations of Statically Unstable Aircraft Due to the Effects of Sensor Noise, Turbulence, and Structural Dynamics," AIAA Guidance, Navigation and Control Conf., AIAA Paper

86-2203, Aug. 1986.

[5]Yamamoto, T., "Impact of Aircraft Structural Dynamics on Integrated Control Design," AIAA Guidance and Control Conf., AIAA Paper 83-2216, Aug. 1983.

[6]Becker, J., Weiss, F., and Sensberg, O., "Compatibility Aspects of Active Control Technologies with Aircraft Structural Design," *Structural Control*, edited by H. H. E. Leipholz, Martinus Nijhoff Publishers, Dordrecht, 1987.

[7]Felt, I. R., Huttsell, J., Noll, T. E., and Cooley, D. E., "Aeroservoelastic Encounters," *Journal of Aircraft*, Vol. 16, No. 7, 1979, pp. 477–483.

[8]Lynch, R. W., and Rogers, W. A., "Aeroelastic Tailoring of Composite Materials to Improve Performance," *Proceedings of the 16th AIAA Structures, Structural Dynamics and Materials Conference*, AIAA, New York, April 1975, pp. 61–68.

[9]Haftka, R. T., "Optimization of Flexible Wing Structures Subject to Strength and Induced Drag Constraints," *AIAA Journal*, Vol. 15, No. 8, 1977, pp. 1101–1106.

[10]Tolson, R. H., and Sobieszczanski-Sobieski, J., "Multidisciplinary Analysis and Synthesis: Needs and Opportunities," AIAA 26th Structures, Structural Dynamics and Materials Conf., AIAA Paper 85-0584, New York, April 1985.

[11]Grossman, B., Gurdal, Z., Strauch, G. J., Eppard, W. M., and Haftka, R. T., "Integrated Aerodynamic/Structural Design of a Sailplane Wing," *Journal of Aircraft*, Vol. 25, No. 9, 1988, pp. 855–860.

[12]Zeiler, T. A., and Weisshaar, T. A., "Integrated Aeroservoelastic Tailoring of Lifting Surfaces," *Journal of Aircraft*, Vol. 25, No. 1, 1988, pp. 76–83.

[13]Morris, S., and Kroo, I., "Aircraft Design Optimization with Multidisciplinary Performance Criteria," *Proceedings of the AIAA/ASME/ASCE/AHS/ASC 30th Structures, Structural Dynamics and Materials Conference*, AIAA Paper 89-1265, Mobile, AL, April 1989, pp. 909–919.

[14]Livine, E., Schmit, L. A., and Friedmann, P. P., "Towards an Integrated Approach to the Optimum Design of Actively Controlled Composite Wings," *Journal of Aircraft*, Vol. 27, No. 12, 1990, pp. 979–992.

[15]Livne, E., Schmit, L. A., and Friedmann, P. P., "Exploratory Design Studies Using an Integrated Multidisciplinary Synthesis Capability for Actively Controlled Composite Wings," 31st Structures, Structural Dynamics and Materials Conf., AIAA Paper 90-0953, Long Beach, CA, April 1990.

[16]Livne, E., "Integrated Multidisciplinary Optimization of Actively Controlled Fiber Composite Wings," Ph.D. Dissertation, Dept. of Mechanical, Aerospace, and Nuclear Engineering, Univ. of California, Los Angeles, CA, Aug. 1990.

[17]Giles, G. L., "Equivalent Plate Analysis of Aircraft Wing Box Structures with General Planform Geometry," *Journal of Aircraft*, Vol. 23, No. 11, 1986, pp. 859–864.

[18]Lynch, R. W., Rogers, W. A., and Braymen, W. W., "Aeroelastic Tailoring of Advanced Composite Structures for Military Aircraft," AFFDL-TR-76-100, Vol. 1, April 1977.

[19]Triplett, W. E., "Aeroelastic Tailoring Studies in Fighter Aircraft Design," *Journal of Aircraft*, Vol. 17, No. 7, 1980, pp. 508–513.

[20]Rogers, W. A., Brayman, W. W., and Shirk, M. H., "Design, Analysis, and Model Tests of an Aeroelastically Tailored Lifting Surface," *Journal of Aircraft*, Vol. 20, No. 3, 1983, pp. 208–215.

[21]Lottati, I., and Nissim, E., "Three Dimensional Oscillatory Piecewise Continuous Kernel Function Method," *Journal of Aircraft*, Vol. 18, No. 5, 1981, pp. 346–363.

[22]Roger, K. L., "Airplane Math Modeling Methods for Active Control Design," *Structural Aspects of Active Controls*, AGARD CP-228, Aug. 1977, pp. 4–11.

[23]Bryson, A. E., and Ho, Y. C., *Applied Optimal Control*, Hemisphere, Washington, DC, Revised Printing, 1975, Chap. 11.

[24]Golub, G. H., Nash, S., and Van Loan, C., "A Hessenberg-Schur Method for the Problem AX + XB = C," *IEEE Transactions on Automatic Control*, Vol. AC-24, No. 6, 1979, pp. 909–913.

[25]McDonald, J. W., and Stevens, J. R., "Optimized Design of Subsonic Lifting Surfaces," *Journal of Aircraft*, Vol. 7, No. 5, 1970, pp. 442–447.

[26]Feifel, W. M., "Optimization and Design of Three-Dimensional Aerodynamic Configurations of Arbitrary Shape by a Vortex Lattice Method," *Vortex Lattice Utilization*, NASA SP-405, 1976, pp. 71–88.

[27]Rajeswari, B., and Prabhu, K. R., "Optimum Flap Schedules and Minimum Drag Envelopes for Combat Aircraft," *Journal of Aircraft*, Vol. 24, No. 6, 1987, pp. 412–414.

[28]Lottati, I., "Induced Drag and Lift of Wing by the Piecewise Continuous Kernel Function Method," *Journal of Aircraft*, Vol. 21, No. 11, 1984, pp. 833, 834.

[29]Wagner, S., "On the Singularity Method of Subsonic Lifting Surface Theory," *Journal of Aircraft*, Vol. 6, No. 6, 1969, pp. 549–558.

[30]Lan, C. E., "A Quasi-Vortex-Lattice Method in Thin Wing Theory," *Journal of Aircraft*, Vol. 11, No. 9, 1974, pp. 518–527.

[31]Schmit, L. A., "Structural Analysis—Precursor and Catalyst," *Recent Experiences in Multidisciplinary Analysis and Optimization*, NASA CP-2327, Pt. 1, 1984, pp. 1–17.

[32]Schmit, L. A., "Structural Optimization—Some Key Ideas and Insights," *New Directions in Optimum Structural Design*, edited by E. Atrek, R. H. Gallagher, K. M. Ragsdell, and O. C. Zienkiewicz, Wiley, New York, 1984.

[33]Haftka, R. T., and Kamat, M. P., *Elements of Structural Optimization*, Martinus Nijhoff, 1985, Chap. 6.

[34]Schmit, L. A., and Miura, H., *Approximation Concepts for Efficient Structural Synthesis*, NASA CR-2552, March 1976.

[35]Starnes, J. H., Jr., and Haftka, R. T., "Preliminary Design of Composite Wings for Buckling, Strength, and Displacement Constraints," *Journal of Aircraft*, Vol. 16, No. 2, 1979, pp. 564–570.

[36]Thomas, H. L., and Schmit, L. A., "Control Augmented Structural Synthesis with Dynamic Stability Constraints," *AIAA Journal*, Vol. 29, No. 4, 1991, pp. 619–626.

[37]Canfield, R. A., "An Approximation Function for Frequency Constrained Structural Optimization," *Recent Advances in Multidisciplinary Analysis and Optimization*, NASA CP-3031, 1989, pp. 937–953.

[38]Thomas, H. L., Sepulveda, A. E., and Schmit, L. A., "Improved Approximations for Control Augmented Structural Synthesis," *AIAA Journal*, Vol. 30, No. 1, 1992, pp. 171–179.

[39]Nissim, E., and Abel, I., "Development and Application of an Optimization Procedure for Flutter Suppression Using the Aerodynamic Energy Concept," NASA TP-1137, Feb. 1978.

[40]Vanderplaats, G. N., *Numerical Optimization Techniques for Engineering Design*, McGraw-Hill, New York, 1984.

[41]Vandeplaats, G. N., "CONMIN—A FORTRAN Program for Constrained Function Minimization: User's Manual," NASA TMX-62,282, Aug. 1973.